J Mater Sci (2009) 44:4117–4123
DOI 10.1007/s10853-009-3597-2

Relationship among the phase equilibria, microstructures, and dielectric properties of $CaCu_3Ti_4O_{12}$ ceramics via different sintering time

Seunghwa Kwon · David P. Cann

Received: 26 March 2009 / Accepted: 14 May 2009 / Published online: 2 June 2009

Abstract The structure–property relationship of the $CaCu_3Ti_4O_{12}$ ceramics processed via conventional solid-state method was studied in terms of the different processing conditions. X-ray diffraction patterns of the tenorite CuO and cuprite Cu_2O secondary phases found on the unpolished and polished surfaces of $CaCu_3Ti_4O_{12}$ were explained by the reduction/reoxidation reaction as a function of sintering time. Based on the microstructures, grain growth of $CaCu_3Ti_4O_{12}$ continued from 0.5 to 4 h sintering while the further growth was limited to the small-sized grains after 8 h sintering. Also, WDS data indicated the Cu-deficient and Ti-excessive stoichiometry of $CaCu_3Ti_4O_{12}$ on both outer and inner regions regardless of sintering time. The change of dielectric constant and tan δ were shortly discussed with regard to the secondary phases and the microstructures of the different sintering hours.

Introduction

Since the discovery of ferroelectric behavior in 1921, it has been one of the major concerns to find out a new class of high dielectric constant (or high K) materials and to develop its processing technology. Most of these high-K materials can be found in the ABO_3-type perovskite ceramic compounds including $BaTiO_3$ [1] and relaxor ferroelectrics such as $Pb(Mg_{1/3}Nb_{2/3})O_3$ [PMN], $Pb(Zn_{1/3}Nb_{2/3})O_3$ [PZN], and $Pb_{1-x}La_x(Zr_{1-y}Ti_y)O_3$ [PLZT] [2]. However, considering the fast growing electronic device technologies due to the miniaturization, high-K ferroelectrics exhibiting the phase transition near Curie temperature are not the ultimate choices. For this reason, a high-K $CaCu_3Ti_4O_{12}$ (CCTO) discovered by Subramanian et al. [3] has drawn huge attraction so far. Based on the previous studies, CCTO has a pseudo-cubic perovskite structure with the space group of *Im3* and the lattice parameter of 7.391 Å [4]. In addition, CCTO has the dielectric constant over 10^4 at room temperature and is temperature independent without any phase transition from 100 to 400 K [5]. In order to explain this unusual dielectric behavior of CCTO, early studies proposed the intrinsic effects in terms of the relaxation modes [5] and the relaxor-like slowing down of the dipole fluctuations [6]. Further reports about the origin of its high K, however, revealed that the abnormality in CCTO might be better elucidated via extrinsic models [7, 8] based on the Maxwell-Wagner relaxation. It is believed that the space charge polarization was induced by an electrically heterogeneous structure in polycrystalline CCTO due to the mobile charged species on the internal interfaces. The internal layer barrier capacitor model suggested by Adams et al. [9] explains the existence of these interfaces consisting of conducting grains and insulating boundaries via impedance analysis, and it became the most widely accepted theory for the abnormal dielectric behavior of CCTO.

The probable explanation for the stoichiometric changes in CCTO during sintering was first given by Li et al. [10]. They suggested that Cu^{2+} reduces to Cu^{1+} upon heating with the substitution of Ti^{4+} on Cu sites, while the reoxidation of Cu^{1+} to Cu^{2+} occurs along with the reduction of Ti^{4+} to Ti^{3+} upon cooling. Following this model, there have been reports dealing with the cation stoichiometry correlated with the dielectric responses, microstructures,

S. Kwon (✉) · D. P. Cann
Materials Science, School of Mechanical, Industrial, and Manufacturing Engineering, Oregon State University, 204 Rogers Hall, Corvallis, Oregon 97331-8569, USA
e-mail: woodie72@gmail.com

and processing conditions of CCTO. Fang et al. [11] showed that the improvement of grain boundary resistivity is due to the existence of Cu-rich grain boundaries. Their subsequent study of EDS analysis confirmed the Cu-rich grain boundaries as well as Cu-deficient grains in CCTO [12]. On the other hand, a study of the variation in Cu content exhibited different aspects from the measured dielectric properties, electrical resistivity, and microstructures by means of the CuO segregation [13]. Recently, a similar research performed by Shri Prakash and Varma [14] reported the effects of the segregation of Cu-rich phase on both dielectric properties and microstructures in terms of the sintering temperatures. Due to the strong dependency of the processing conditions on the dielectric properties and microstructures [15, 16], however, the clear mechanism about the stoichiometric changes in CCTO has not been settled yet. Continued from our previous study about the different sintering temperature effects [17], current research is focused on the relationship between property and structure in CCTO via different sintering time. Since the optimum dielectric response was obtained at a sintering temperature of 1115 °C [17], all sintering profiles in this study were fixed at this temperature. The results obtained from the XRD data, dielectric measurements, and chemical composition analysis via an electron probe micro-analyzer are discussed for the understanding of structure–property–process relationship in CCTO.

Experimental

The ceramic processing to obtain stoichiometric $CaCu_3Ti_4O_{12}$ powder was carried out through the conventional solid-state synthesis. First, highly pure (>99.9%) $CaCO_3$, CuO, and TiO_2 powders were mixed from the batch calculation. Then, the powder was milled in ethanol with yttria-stabilized ZrO_2 media for 6 h by using a vibratory mill (SWECO, Florence, KY). After completion, the powder was calcined at 1000 °C in air for 24 h in order to obtain homogeneous CCTO powder. For the proof of phase stability, calcined CCTO powder was examined via an X-ray diffractometer (Bruker D8 Discover, Germany). Following the second milling of the calcined CCTO powder, green pellets of CCTO (diameter of 12.7 mm) were made by using a cold uniaxial press (Carver Press Inc.) with approximately 3 wt% of organic binder. All green CCTO pellets were fired at 1115 °C in air for different sintering hours (0.5, 1, 2, 4, 8 h) with the heating rate of 5 °C/min followed by air quenching. With these sintered pellets, both unpolished (i.e., outer surface) and polished (i.e., inner region) surfaces were investigated via X-ray diffraction (XRD). For the dielectric measurements, both bottom and top surfaces of each CCTO pellet were coated from the Au target in a sputtering unit (ScanCoat 6, Edward, UK) as electrodes. And the dielectric constant and dielectric loss (tan δ) were measured as a function of frequency between 100 Hz and 1 MHz via an LCR meter (Model 4284A, Agilent) at room temperature. For the further study about the stoichiometry–microstructure–dielectric property relationship, an electron probe micro-analyzer (SX-100, Cameca) was utilized to obtain the chemical compositions of both unpolished and polished surfaces on 0.5, 4, and 8 h sintered CCTO.

Results and discussion

The XRD data of unpolished CCTO samples sintered at 1115 °C for different hours (0.5, 1, 2, 4, and 8 h CCTO, hereafter) are plotted in Fig. 1. All patterns are well matched with the major CCTO peaks based on the Powder Diffraction File database (#75-2188). However, three minor peaks are found in an extended pattern from 30° to 55° shown as Fig. 2. Peaks near 35.5° and 38.8° were identified as the CuO (tenorite) phase and they appeared on all CCTO pellets regardless of the sintering time, whereas another little peak around 36.5° was formed as a Cu_2O (cuprite) phase. Unlike the CuO, this Cu_2O phase was seen on 0.5, 1, and 2 h CCTO but disappeared on 4 and 8 h CCTO.

As a quantitative analysis, intensity ratios of each CuO and Cu_2O to the maximum CCTO peak at 34.3° were presented in Table 1 and plotted in Fig. 3. Here, the ratio of CuO to CCTO (i.e., I_{CuO}/I_{CCTO}) on the unpolished surface increases with the sintering time up to 4 h with the maximum value of 0.0615, then decreases to 0.0333 on 8 h CCTO. In contrast to the case of CuO, the intensity ratio of

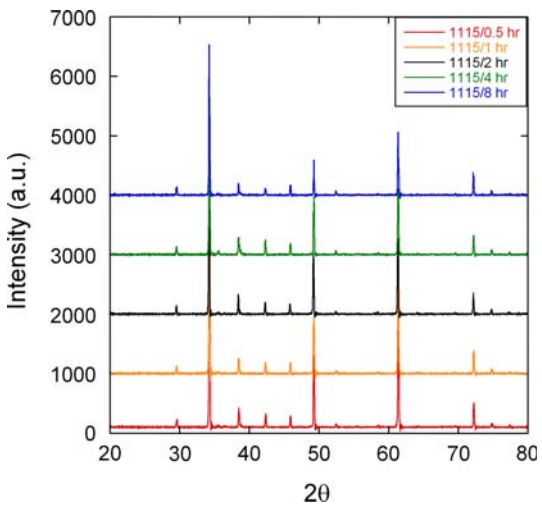

Fig. 1 A plot of XRD patterns of the CCTO samples (unpolished) in terms of different sintering time

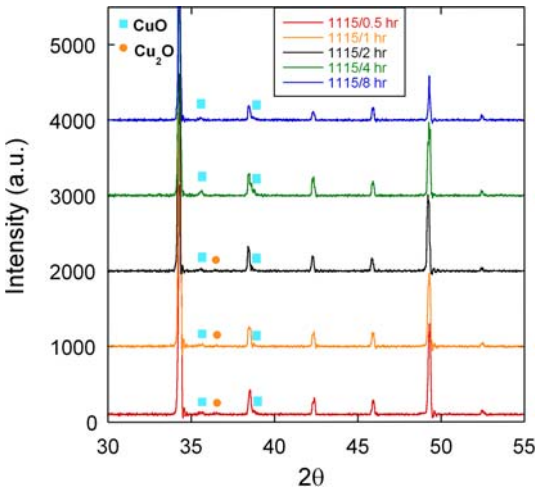

Fig. 2 A plot of extended XRD patterns in the range of 30–55° of Bragg angle with the secondary phases in CCTO samples of different sintering time

Table 1 Intensity ratios and lattice parameters of CCTO pellets with different sintering time

	Sintering time (hours)				
	0.5	1	2	4	8
I_{CuO}/I_{CCTO} (unpolished)	0.0287	0.0269	0.0429	0.0615	0.0333
I_{Cu_2O}/I_{CCTO} (unpolished)	0.0096	0.0084	0.0092	0.0077	0.0040
I_{Cu_2O}/I_{CCTO} (polished)	0.0224	0.0197	0.0137	0.0160	0.0096
Lattice parameter (Å)	7.3925	7.3900	7.3964	7.3961	7.3966

Cu_2O to CCTO (i.e., I_{Cu_2O}/I_{CCTO}) remains similar among the unpolished surfaces of CCTO sintered between 0.5 and 4 h but decreases to 0.004 on 8 h CCTO. Based on the XRD data of the polished CCTO samples where only Cu_2O was found as a secondary phase (not shown), Fig. 3 also indicates that the calculated I_{Cu_2O}/I_{CCTO} decreases with the sintering time. The measured lattice parameters of CCTO increase up to 2 h of sintering and remain nearly constant for 2, 4, and 8 h CCTO.

The intensity ratios of secondary phases as a function of sintering time can be explained from the following ways. Upon heating, reduction from CuO to Cu_2O in CCTO results in the coexistence of both phases on the unpolished surfaces of CCTO samples. When CCTO samples were under rapid cooling, the reoxidation occurs on the surfaces of CCTO samples by changing some Cu_2O to CuO. On the other hand, our previous results from TG/DTA measurements indicated the possibility of Cu volatility at the sintering temperature over 1100 °C [18]. Since it is not clear whether the volatility of Cu is originated from CuO and/or Cu_2O, the trend of changes in I_{CuO}/I_{CCTO} and I_{Cu_2O}/I_{CCTO} on the surface of CCTO may not be well explained as a function of sintering time. In case of the inner regions of CCTO, more sintering time will continuously change CuO to Cu_2O by the reduction reaction. Consequently, the Cu_2O-rich portion inside the CCTO pellet expands and the outer region containing both CuO and Cu_2O becomes narrower. Upon rapid cooling (i.e., quenching), Cu_2O formed on the outer surface tends to be reoxidized to CuO, which explains the increasing amount of CuO with the sintering time up to 4 h. The gradual decrease in I_{Cu_2O}/I_{CCTO} with the sintering time on the polished CCTO surface can be traced from the aforementioned Cu volatility. In contrast, the reoxidation from Cu_2O to CuO on the inner region of CCTO is prevented by the limited oxygen diffusion during the rapid cooling regardless of the previous sintering time, resulting in the decrease of I_{Cu_2O}/I_{CCTO} ratio with the sintering time. Judging from the very small intensity ratios (0.0096–0.0224) as well as the complex reactions by the dynamic motions of Cu and O, further

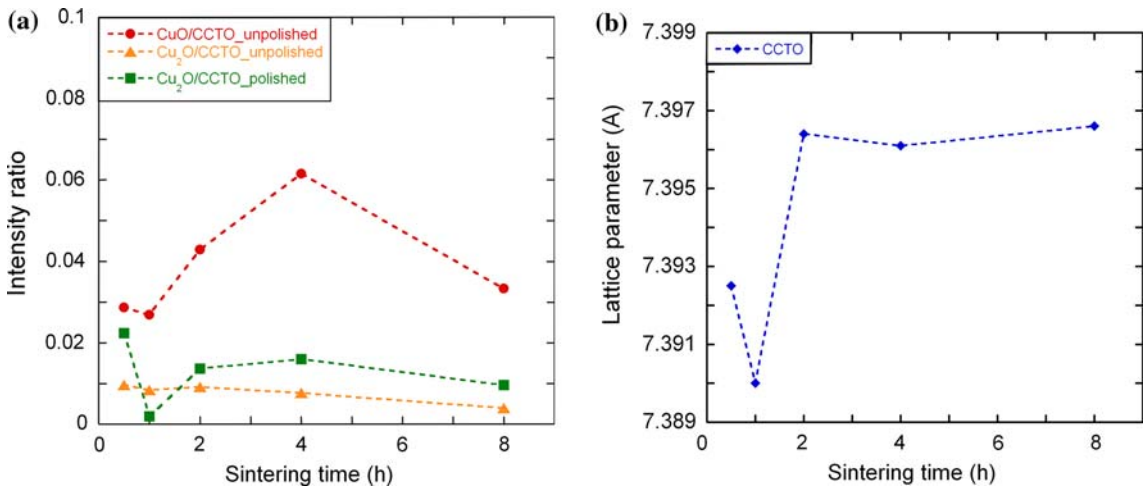

Fig. 3 Plots of **a** the intensity ratio of Cu_2O to CCTO and **b** the lattice parameter of CCTO samples as a function of sintering time

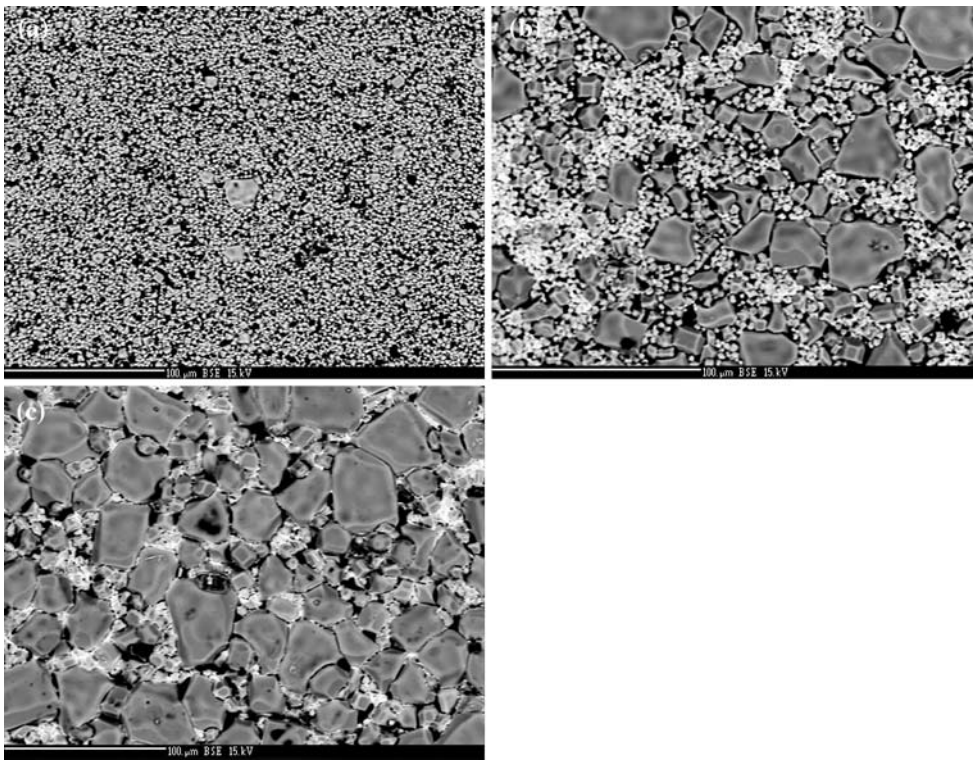

Fig. 4 Micrographs of the unpolished CCTO samples sintered for **a** 0.5 h, **b** 4 h, and **c** 8 h via electron probe micro-analyzer

detailed research about the kinetics of the secondary phases in CCTO is necessary to clarify the results shown here through the layer-by-layer examination.

The electron probe micro-analyzer micrographs of unpolished CCTO samples sintered at 1115 °C are shown in Fig. 4. The micrograph of 0.5 h CCTO plotted in Fig. 4a shows the few large-sized grains that grow from the tiny grains and few large grains. When the sintering time increased up to 4 h, the microstructure clearly indicates the grain growth and consists of two different regions in Fig. 4b: the larger grains (dark colored) are surrounded by very small grains (bright colored). Further increase of the sintering time up to 8 h shows that grain growth continues from these small-sized grains, reducing the bright regions. It seems that the growth rate of large grains from 4 to 8 h CCTO decreased. As it will be introduced later in this report, the measured dielectric constant increases with the sintering time over 10 kHz. Therefore, there is no direct relationship between the grain size and the dielectric constant. Aygün et al. [19] reported the similar results and explained that these discrepancies might be attributed to the compositional changes in CCTO. In order to further examine the chemical compositions of grains, wavelength dispersive X-ray spectroscopy (WDS) was performed for 0.5, 4, and 8 h CCTO and the resulting stoichiometric ratios of Cu/Ca and Ti/Ca are plotted in Fig. 5 (Note that Ca stoichiometry was normalized as 1.0). Based on the average values indicated inside the error ranges, Cu becomes deficient (i.e., Cu_{3-x}) in CCTO regardless of the sintering time in Fig. 5a while Ti stoichiometry remains excessive (i.e., Ti_{4+x}) as seen in Fig. 5b. It is interesting to find that there are relatively large errors of Cu and Ti stoichiometry for 0.5 h CCTO. Also, the WDS data revealed much higher Cu content on the smaller grains of 4 and 8 h CCTO (not shown). Since the grain growth of CCTO is at the initial stage after 0.5 h sintering, this large error might come from the Cu-rich small-sized grains.

On the other hand, micrographs of the polished surface of 0.5, 4, and 8 h CCTO presented in Fig. 6 reveal the similar aspect to the case of the unpolished surfaces. Although the clear grain structure is not available (i.e., samples are not thermally etched at the elevated temperature), the analogous growth patterns can be seen from the microstructures of 0.5, 4, and 8 h CCTO. This result is in accordance with the scanning electron micrographs of CCTO pellets sintered at 1100 °C for 2.5–20 h, reported by Shri Prakash and Varma [14]. In contrast to the plots of Cu and Ti stoichiometry for unpolished CCTO, stoichiometric ratios obtained from the polished surfaces and plotted in Fig. 7 have relatively smaller error ranges. In addition, the Cu deficiency (Fig. 7a) and Ti excess (Fig. 7b) on the polished surface of CCTO pellets were found regardless of the sintering time. The change from the stoichiometric to Cu-poor and Ti-rich CCTO over the entire regions after the rapid cooling was proved via the additional WDS data (not shown here) measured on the cross sections of 0.5, 4, and 8 h CCTO pellets from 0 μm (unpolished surface) to 800 μm (center of the sample).

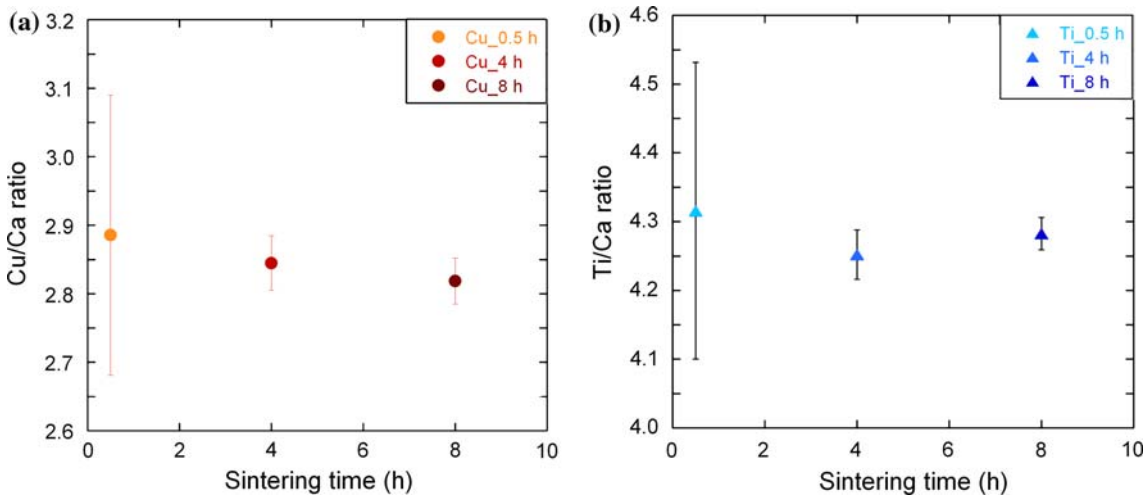

Fig. 5 Plots of the **a** Cu/Ca and **b** Ti/Ca stoichiometric ratio of the unpolished CCTO samples as a function of sintering time

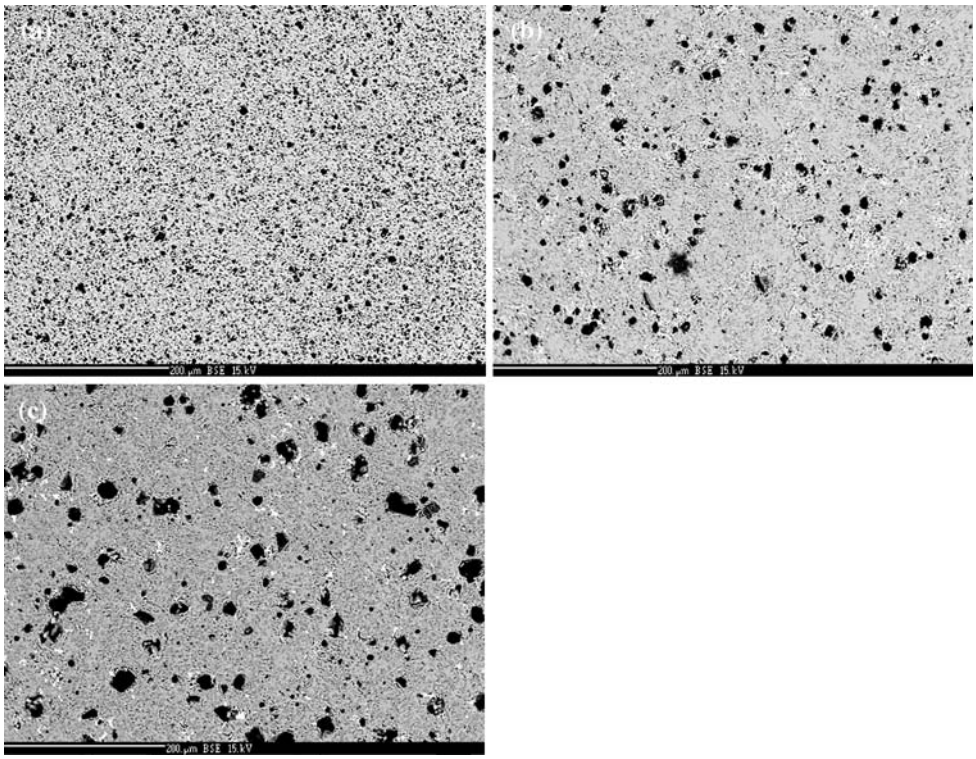

Fig. 6 Micrographs of the polished CCTO samples sintered for **a** 0.5 h, **b** 4 h, and **c** 8 h via electron probe micro-analyzer

The room temperature dielectric constant and the loss tangent of the CCTO pellets measured as a function of frequency are shown in Figs. 8 and 9, respectively. The dielectric response of CCTO exhibits strong frequency dependence due to the space charge polarization that results from an electrically heterogeneous microstructure. In Fig. 8, the dielectric constant of CCTO samples increased with the sintering time at the frequencies over 10 kHz. Since the dielectric constant in a barrier layer capacitor is governed by the ratio of the overall thickness of material to the barrier layer (i.e., $h_o/2$ h) [2], it is reasonable that the 8 h CCTO with the thinnest barrier layer shows the highest dielectric constant. Similar trend can also be found in the dielectric loss data shown in Fig. 9. Here, tan δ rises when the sintering time increases from 2 to 8 h. Compared to 1 and 2 h CCTO samples, however, anomalously large dielectric constant ($f = 100$ Hz–10 kHz) and tan δ ($f <$ 100 kHz) were shown in Figs. 8 and 9, respectively. These deviations observed in the loss tangent of 0.5 h CCTO might be linked to its unstable microstructure where the

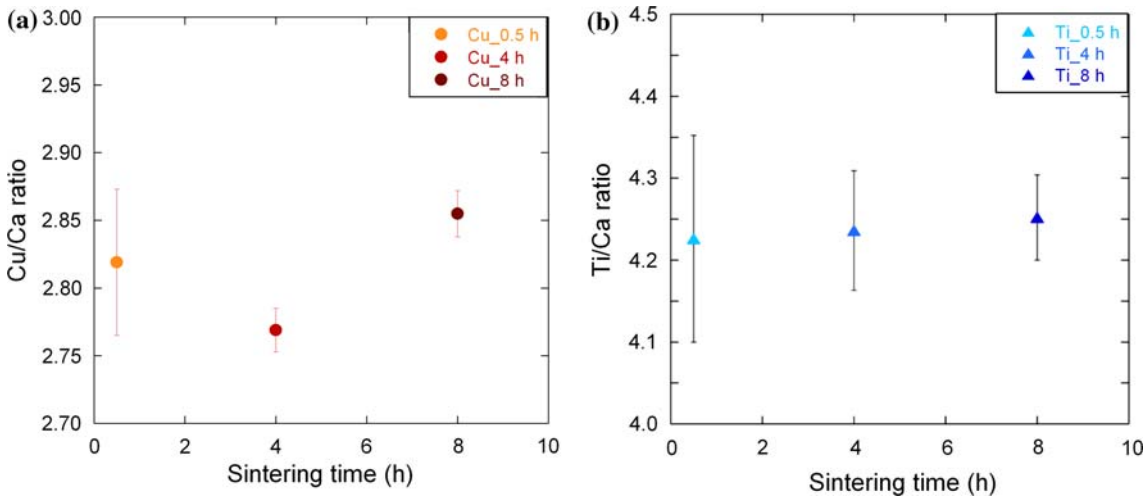

Fig. 7 Plots of the **a** Cu/Ca and **b** Ti/Ca stoichiometric ratio of the polished CCTO samples as a function of sintering time

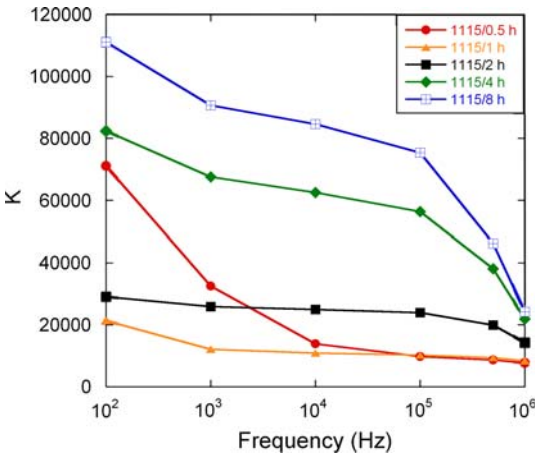

Fig. 8 Plots of the dielectric constant versus frequency of the polished CCTO samples with different sintering time at 1115 °C

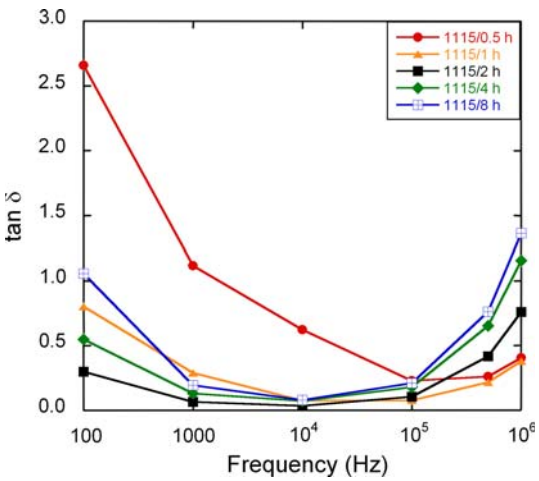

Fig. 9 Plots of the loss tangent (tan δ) versus frequency of the polished CCTO samples with different sintering time at 1115 °C

growth of CCTO grains was limited by the lack of sintering time followed by the rapid cooling, creating more Cu-rich boundary regions which contributes to the higher loss. These dielectric loss values are relatively low, but higher than those typically obtained for doped CCTO such as 0.5 mol% ZrO_2-added CCTO which has tan δ values below 0.05 over these frequencies [20]. Lastly, it is worth noting that the dielectric constant of 8 h CCTO pellet shows the maximum value around $K \sim 84{,}600$ at 1 kHz while its tan δ marks as low as 0.08 at the same frequency.

Conclusions

The phase equilibria, microstructures, and the dielectric properties of CCTO pellets were investigated in terms of the sintering time. X-ray diffraction data revealed that the calculated intensity ratio of I_{CuO}/I_{CCTO} and I_{Cu_2O}/I_{CCTO} could explain the secondary phases as a function of sintering time based on the reduction/reoxidation reactions. The microstructures of unpolished and polished surfaces of CCTO showed the continuous grain growth from 0.5 to 8 h sintering, but the rate of growth decreased after 4 h of sintering. In addition, the WDS data confirmed that the stoichiometry of the quenched CCTO is deficient in Cu and excessive in Ti on both the outer surface and the inner region regardless of sintering time. From the dielectric measurements, both dielectric constant and loss tangent increase with the amount of sintering time. The highest dielectric constant obtained from 8 h CCTO can be attributed to the reduced barrier layer thickness surrounding Cu_2O-rich inner regions. The deviation of tan δ on 0.5 h CCTO at low frequencies might be related to the large area of Cu-rich boundary regions shown from the microstructure.

Acknowledgements This work was supported by the Office of Naval Research Capacitor Program and the American Chemical Society's Petroleum Research Foundation. Also, authors are thankful to Dr. Frank J. Tepley III at Oregon State University for his support from the electron microprobe analysis.

References

1. Bhalla AS, Guo R, Roy R (2000) Mater Res Innov 4:3
2. Moulson AJ, Herbert JM (2003) Electroceramics, 2nd edn. Wiley, Chichester
3. Subramanian MA, Li D, Duan N, Reisner BA, Sleight AW (2000) J Solid State Chem 151:323
4. Bochu B, Deschizeaux MN, Joubert JC, Collomb A, Chenavas J, Marezio M (1979) J Solid State Chem 29:291
5. Ramirez AP, Subramanian MA, Gardel M, Blumberg G, Li D, Vogt T, Shapiro SM (2000) Solid State Commun 115:217
6. Homes CC, Vogt T, Shapiro SM, Wakimoto S, Ramirez AP (2001) Science 293:673
7. He L, Neaton JB, Cohen MH, Vanderbilt D, Homes CC (2002) Phys Rev B 65:214112
8. Lunkenheimer P, Bobnar V, Pronin AV, Ritus AI, Volkov AA, Loidl A (2002) Phys Rev B 66:052105
9. Adams TB, Sinclair DC, West AR (2002) Adv Mater 14(18): 1321
10. Li J, Subramanian MA, Rosenfeld HD, Jones CY, Toby BH, Sleight AW (2004) Chem Mater 16:5223
11. Fang TT, Mei LT, Ho HF (2006) Acta Mater 54:2867
12. Fang TT, Mei LT (2007) J Am Ceram Soc 90:638
13. Shao SF, Zhang JL, Zheng P, Wang CL (2007) Solid State Commun 142:28
14. Shri Prakash B, Varma KBR (2007) J Mater Sci 42:7467. doi: 10.1007/s10853-006-1251-9
15. Ni WQ, Zheng XH, Yu JC (2007) J Mater Sci 42:1037. doi: 10.1007/s10853-006-1431-7
16. Almeida AFL, Fechine PBA, Kretly LC, Sombra ASB (2006) J Mater Sci 41:4623. doi:10.1007/s10853-006-0052-5
17. Kwon S, Cann DP (in press) J Electroceram. doi:10.1007/s10832-009-9563-1
18. Kwon S, Triamnak N, Cann DP (2008) In: Proceedings of the 17th international symposium on applications of ferroelectrics, Santa Fe, NM
19. Aygün S, Tan X, Maria JP, Cann DP (2005) J Electroceram 15:203
20. Kwon S, Huang CC, Patterson EA, Alberta EF, Kwon ST, Hackenberger WS, Cann DP (2008) Mater Lett 62:633